Numerical modeling of the development of intermetallic layers between aluminium and steel during co-extrusion

Cite as: AIP Conference Proceedings **2113**, 040029 (2019); https://doi.org/10.1063/1.5112563
Published Online: 02 July 2019

B.-A. Behrens, C. Klose, S. E. Thürer, N. Heimes, and J. Uhe

Numerical Modeling of the Development of Intermetallic Layers between Aluminium and Steel during Co-Extrusion

B.-A. Behrens[1, a)], C. Klose[2, b)], S. E. Thürer[2, c)], N. Heimes[1, d)] and J. Uhe[1, e)]

[1]*Institut für Umformtechnik und Umformmaschinen (Forming Technology and Machines), Leibniz Universität Hannover, An der Universität 2, 30823 Garbsen, Germany*

[2]*Institut für Werkstoffkunde (Materials Science), Leibniz Universität Hannover, An der Universität 2, 30823 Garbsen, Germany*

[a)] behrens@ifum.uni-hannover.de
[b)] klose@iw.uni-hannover.de
[c)] thuerer@iw.uni-hannover.de
[d)] nheimes@ifum.uni-hannover.de
[e)] Corresponding author: uhe@ifum.uni-hannover.de

Abstract. Undergoing the Tailored Forming process chain, coaxial aluminium-steel profiles joined by co-extrusion are formed into hybrid bearing bushings by die forging. During the joining of aluminium and steel, intermetallic phases may develop. As these phases are very hard and brittle, it is important to be able to predict the width of the resulting intermetallic layer because it is likely to reduce the strength of the compound for the subsequent forging step. In the scope of this paper, a possibility for numerical calculation of the resulting phase thickness during the co-extrusion of aluminium and steel, by means of Lateral Angular Co-Extrusion (LACE), is presented. In the first step, an analogy test on a forming dilatometer was developed for the experimental investigation of the intermetallic phase formation. The width of the intermetallic phase seam was determined by means of scanning electron microscopy using an image processing tool. Based on the experimental results, a calculation instruction was defined to describe the intermetallic phase thickness as a function of temperature and contact time. The function was implemented in a commercial finite element (FE) software by means of a user-defined subroutine and validated on the basis of experimental data.

INTRODUCTION

These days, requirements for technical components increase. Therefore, components with low weight, compact design and enhanced functionality are required. Hence, the use of mono-material components is not sufficient to meet these requirements in some applications. Using a combination of different materials in one component enables properties, which are locally adapted to the occurring loads. At present, hybrid solid components are joined during or after the forming process. The Collaborative Research Centre (CRC) 1153 deals with the development of novel process chains for the manufacture of hybrid solid components by "Tailored Forming". In the case of Tailored Forming, hybrid semi-finished workpieces, which consist of two or more different materials, are joined prior to the main forming process. The process chain discussed in this study starts with a Lateral Angular Co-Extrusion (LACE) process for the coaxial combination of the aluminium alloy EN AW-6082 and the case-hardening steel 20MnCr5. In a subsequent die forging process, hybrid bearing bushings with a wear-resistant sliding surface are formed. Following, a heat treatment to realise locally adapted material properties and a finishing process by machining take place. The process chain is accompanied by numerical simulations for process design and prediction of the joining zone properties.

Proceedings of the 22nd International ESAFORM Conference on Material Forming
AIP Conf. Proc. 2113, 040029-1–040029-6; https://doi.org/10.1063/1.5112563
Published by AIP Publishing. 978-0-7354-1847-9/$30.00

The combination of aluminium and steel by co-extrusion is well-known in literature and an object of research for decades. In subproject A1 of the CRC 1153 a LACE process is employed which combines co-extrusion with conventional billets and Equal Channel Angular Pressing (ECAP). Due to the redirection of the billet material in an ECAP die, a stronger deformation of the billet material takes place. Thus, ECAP enables grain refinement. During the LACE process the reinforcement is fed laterally to the matrix material within the deformation zone. Grittner et al. developed a LACE process for the combination of aluminium and titan [1]. In [2] the LACE process for the production of hybrid aluminium-steel profiles is presented. In style of Grittner et al., the aluminium billet is redirected in the extrusion die at an angle of 90°.

A decisive factor of the quality of hybrid profiles is the joining zone, due to the formation of intermetallic phases (IMP). Aluminium and iron are hardly soluble in each other in the solid state. The maximum solubility of iron in aluminium is only about 0.03 % at the eutectic temperature of 655 °C [3]. Depending on the ratio of iron to aluminium, different intermetallic compounds can develop. From the binary Fe-Al phase diagram two superstructures and four intermetallic phases are derived, see Fig. 1. Typically, intermetallic compound layers consisting of $FeAl_3$ and Fe_2Al_5 are formed by diffusion processes. Intermetallic phases have complex atomic structures which strongly inhibit dislocation movements and lead to high hardness values. Due to the low mobility of the dislocations, intermetallic phases generally exhibit a very brittle material behaviour [4, 5].

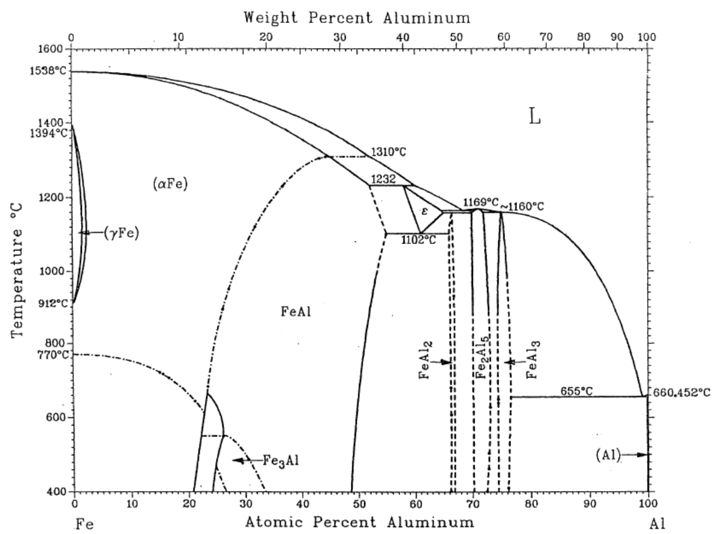

FIGURE 1. Fe-Al phase diagram [6]

An indispensible aspect in assessing the strength of hybrid components made of aluminium and steel is the thickness of the intermetallic phase seam. In literature, a phase seam thickness of up to 10 µm is considered sufficiently strong by Springer et al., i.e. the strength of the compound corresponds to that of the weaker joining partner, in this case aluminium [7]. Laukant indicates a tolerable layer thickness of 6-12 µm [4]. According to Yamamoto et al. intermetallic phases can already cause a decrease in strength of the compound from a phase seam thickness of 5-10 µm and should therefore be avoided [8]. However, a sufficiently thin intermetallic phase seam can even improve the strength of the joining zone. In workpieces produced by friction welding, a layer thickness from 0.2-1.0 µm is considered to be beneficial for the joining zone properties [9].

According to Jank et al., the growth of intermetallic phases can be divided into individual sections, as shown schematically in Fig. 2 [10]. The first areas of an intermetallic phase (2) are created by diffusion processes at the bordering elements (1). These areas develop along the joining zone (3) and finally grow together (4). By growing together, the second phase begins, in which the intermetallic phase continues to grow transversely to the joining zone (5). An intermetallic phase seam is usually composed of several subphases (6). The thickness of the intermetallic phases is particularly influenced by the diffusion time and the joining temperature [11]. It is described in literature that the layer thickness growth follows a parabolic function with increasing time. It is also known that a significantly thinner phase seam is formed in solid state joining processes compared to fusion welding [7].

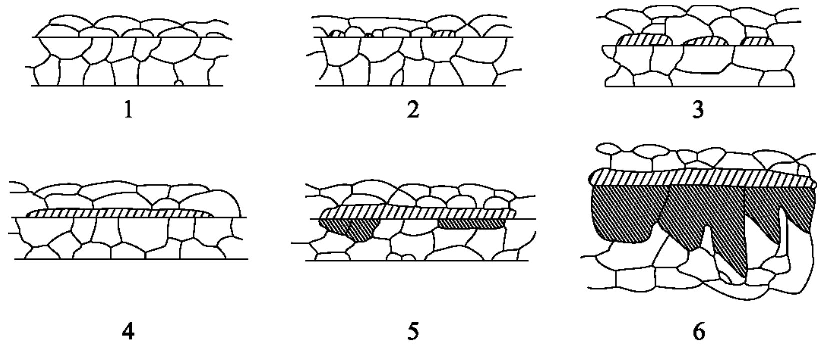

FIGURE 2. Schematic description of the growth of intermetallic phases [10]

In the present study a subroutine is developed to describe the resulting intermetallic phase seam thickness during the co-extrusion process. Therefore, model tests on a forming dilatometer are developed and carried out with different forming temperatures to generate an experimental database for the numerical investigations.

EXPERIMENTAL INVESTIGATIONS

The experiments described in this study were carried out on a quenching and forming dilatometer. In order to analyse and quantify the development of intermetallic phases in the described co-extrusion process, aluminium and steel specimens were compressed considering the relevant boundary conditions of the co-extrusion process such as temperature, pressure and holding time. First investigations showed the presence of an aluminium oxide layer between the deformed aluminium and the steel cylinder, but no intermetallic phases were detected. Thus, an elimination of the oxide layer was performed using modified geometries in the subsequent experiments [12]. With these modified geometries, the aluminium oxide layer was sheared off because of the large deformation of the aluminium, which resembles the conditions present in the LACE-process. Based on these results, it was decided to use the experimental setup shown in Fig. 3 a) for the following investigations. A cylindrical aluminium sample with a diameter of 3 mm is placed between two steel samples with a diameter of 5 mm. A steel sleeve was used to prevent the aluminium sample from being squeezed out between the steel samples and to obtain higher stresses than the yield stress of aluminium. In order to ensure that no oxide layer is present over the entire surface, the samples were additionally grinded and polished before the experiments. The specimens were heated up by inductive heating and held at a constant temperature to achieve a homogeneous temperature distribution and subsequently pressed with a defined constant force. After a given period of time, the specimens were quenched with nitrogen. The force-time and temperature-time curve of the experiments is exemplarily shown in Fig. 3 b).

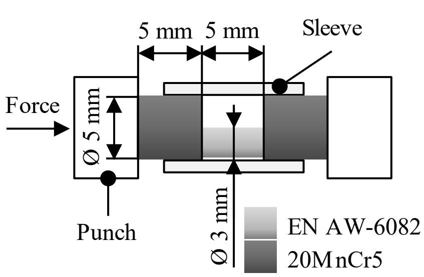

(a)

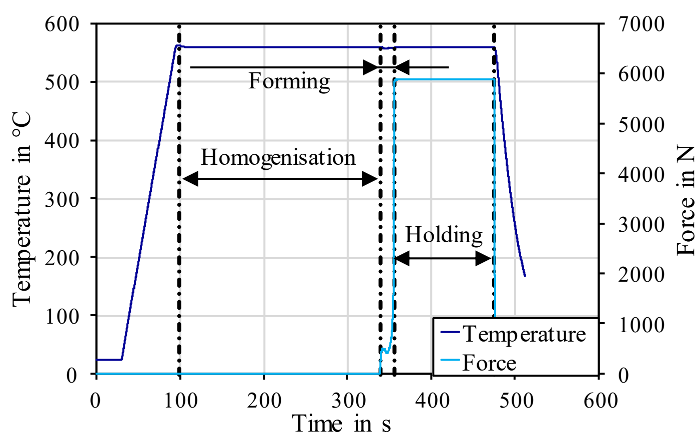

(b)

FIGURE 3. (a) Schematic test set up, (b) exemplary force-time and temperature-time curves

In order to meet the conditions of the LACE process the parameters of the described model experiments were determined based on numerical simulations. Therefore, numerical simulations with different extrusion parameters such as ram speed, temperature and extrusion ratio were carried out to determine the particular temperature, contact pressure and contact time between aluminium and steel. For the numerical investigations, the commercial FEA system FORGE NxT 1.1 was used to simulate the extrusion process. The numerical model and its validation are described in [13].

For the microstructural investigations, the specimens of the dilatometer experiments were prepared metallographically normal to their longitudinal axis. The interface was analysed by scanning electron microscopy (SEM) with energy dispersive X-ray spectroscopy (EDS) using a Supra 40VP from Zeiss. Images were recorded using secondary and backscattered electrons. The results of the SEM analysis of the described experiments conducted in the dilatometer for different forming temperatures are shown in Fig. 4. As shown in Fig. 4 a), no intermetallic phase seam was observed for a forming temperature of 450 °C. For a forming temperature of 505 °C intermetallic phases were detected, which existed as isolated islands in the joining zone (Fig. 4 b). A constant band of intermetallic phases was detected at a forming temperature of 560 °C, see Fig. 4 c). The width of the continuous phase seam is also significantly larger than that of the specimen formed at 505 °C. As can be seen in Fig. 4 d), the intermetallic phase fringe continues to grow with a further increase in temperature to 590 °C. The intermetallic phase seam is of such size that different gray scales can be detected within the phase, indicating the presence of different intermetallic phases within the joining zone. This correlates with the phase grow mechanism described by [10]. The recorded SEM images were evaluated afterwards using a MATLAB script developed by Herbst et al. [14]. The script is used to determine the intermetallic phase based on the different shades of grey of the SEM images and then calculate the width of the phase over the number of pixels. Either the minimum or maximum value of the phase thickness can be determined, or the mean value can be calculated. The function and procedure of the script is described in detail in [14]. In the SEM images described above, intermetallic phase seam widths between 0.3 µm and 6 µm were determined using the backscattered electron detector (BSD). As mentioned in [9], the brittle intermetallic phases should be rather thin to maintain the strength of the bond at the interface. For the intended application this is of outstanding importance as the hybrid profiles need to withstand the subsequent die forging process.

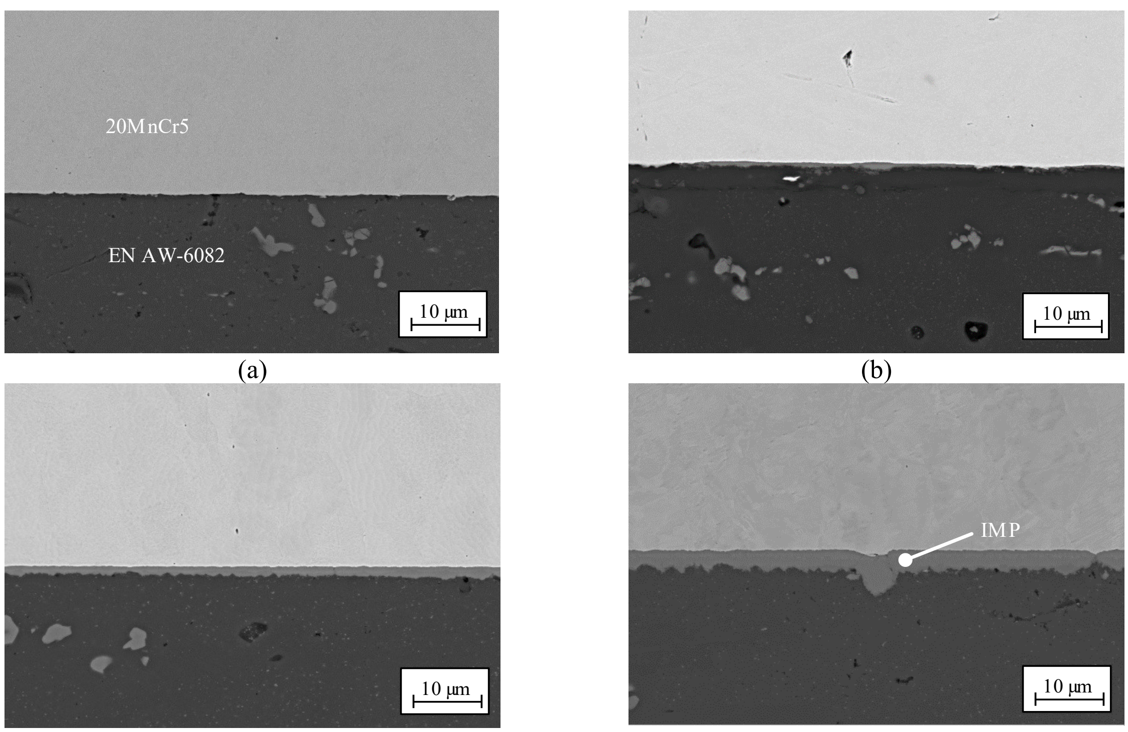

(a) (b) (c) (d)

FIGURE 4. Influence of the temperature on formation of intermetallic phases for a holding time of 120 s; a force of 5890 N and a temperature of (a) 450 °C, (b) 505 °C, (c) 560 °C (d) 590 °C

NUMERICAL MODELLING

The formation and growth of intermetallic phases in the solid state is determined by the diffusion that occurs and which can be described by the 1st and 2nd Fick's Law. In order to use Fick's law, the concentration gradient between the diffusion partners must be known, which could not be determined in the context of this investigation.

Another way to mathematically describe the diffusion or the diffusion distance is the Einstein-Smoluchowski equation (Equation 1). The equation describes the diffusion distance p after a diffusion time t. The diffusion velocity is described by the diffusion coefficient D. The diffusion coefficient indicates how many atoms diffuse through the contact surface over the time t.

$$p = \sqrt{2Dt} \quad \text{Eq. 1}$$

The phase thicknesses p which were determined from the SEM images were used to calculate the diffusion coefficient D with the Einstein-Smoluchowski equation. The diffusion coefficient was calculated for different temperatures. The intermetallic mean phase width for investigated temperatures is shown in Fig. 5 a). It can be seen that the phase width increases exponentially with increasing temperature. The diffusion coefficient calculated in dependency on the temperature is also shown in Fig. 5 a) and has a similar course as the intermetallic phase thickness. The diffusion coefficient at a temperature of 560 °C is $D = 5.16\text{E}^{-15}$ m^2/s and differs from the diffusion coefficient of $D = 8.8\text{E}^{-15}$ m^2/s given by Rummel et al. at a temperature of 555 °C [15]. The difference is caused by the different experimental set-ups and procedures. Rummel et al. investigated the diffusion coefficients of Fe-3d-transition elements in aluminium single crystals in order to eliminate the interfering influences of the oxide layer. For this reason the given diffusion coefficient is above the values determined in this paper. Based on these findings a subroutine was developed to numerically model and visualize the intermetallic phase seam. Based on the experimentally determined diffusion coefficients, the subroutine calculates and summarises the phase size at each time step. In order to use the correct diffusion coefficient in the simulation for temperatures between the experimentally investigated values, an approximation for the temperature range of 450 °C to 590 °C was obtained using the calculated diffusion coefficients and implemented in the subroutine.

In order to verify the functionality of the subroutine, the dilatometer test was simulated first and the calculated phase width was compared with the experimental results. Fig. 5 b) shows the FE model of the dilatometer test carried out for a temperature of 560 °C, a holding time of 120 s and a force of 5890 N. The resulting variable, visualised as a color plot in the FE model, is the mean intermetallic phase width calculated in the contact area between the aluminium and steel specimens. The calculated mean phase width is $p = 1.19$ µm and reproduces very well the mean intermetallic phase width of the experimental tests with $p = 1.20$ µm.

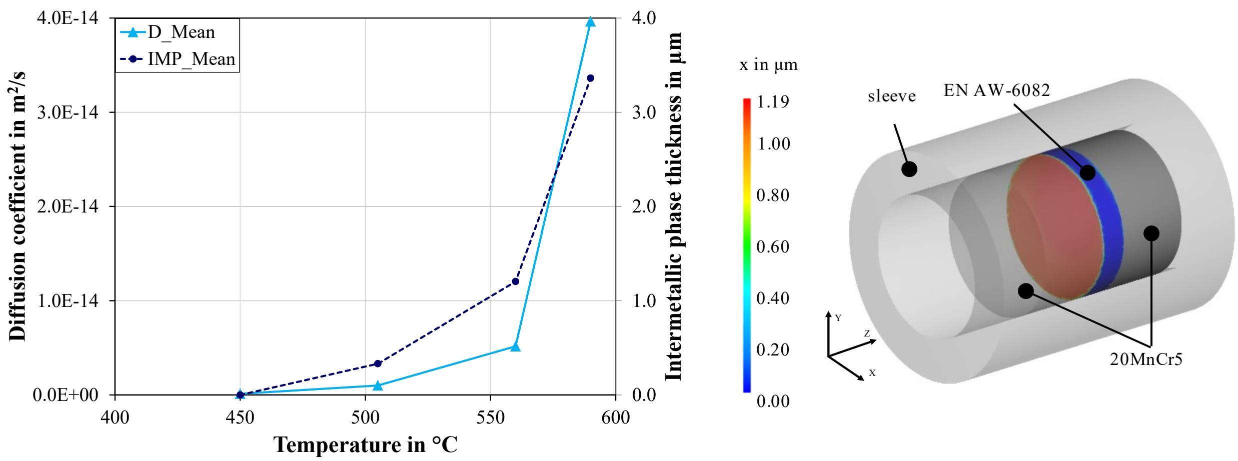

(a) (b)

FIGURE 5. (a) Calculated diffusion coefficient and experimental measured intermetallic phase seam thickness for different temperatures, (b) simulated intermetallic phase thickness in dilatometer experiment for $T = 560$ °C, $t = 120$ s, $F = 5890$ N

SUMMARY AND OUTLOOK

Within the scope of this work, the development of a subroutine to calculate the intermetallic phase seam thickness was presented. First, an experimental setup was designed for model tests on a forming dilatometer and experiments were carried out at different temperatures to determine the influence of the temperature on the resulting phase width. The thickness of the resulting intermetallic phases was subsequently determined using SEM examinations and optical image analysis. The associated diffusion coefficients were calculated using the Einstein-Smoluchowski equation. With rising temperature, an increase of the phase width and the diffusion coefficient could be observed. The developed calculation rule was implemented into the commercial FE-software Forge NxT by means of a subroutine. As a first step, the functionality of the subroutine was tested by simulating the model experiments and a good agreement with the experimental results was determined.

In future work, further experimental investigations will be carried out to determine the influence of other boundary conditions, such as force, on the diffusion coefficient and the resulting intermetallic phase seam. In addition, the usability of the subroutine for the co-extrusion process will be tested and validated by means of corresponding experimental investigations.

ACKNOWLEDGMENTS

The results presented in this paper were obtained within the Collaborative Research Centre 1153 "Process chain to produce hybrid high performance components by Tailored Forming" in the subproject A1, funded by the Deutsche Forschungsgemeinschaft (DFG, German Research Foundation) - 252662854. The authors would like to thank the German Research Foundation for the financial support of this project.

REFERENCES

1. N. Grittner, B. Striewe, A. V. Hehl, D. Bormann, M. Hunkerl, H. W. Zoch and F. W. Bach, Key Eng. Mater. **491**, 67–74 (2012).
2. S. E. Thürer, J. Uhe, O. Golovko, C. Bonk, A. Bouguecha, B.-A. Behrens and C. Klose, Key Eng. Mater. **742**, 512–519, (2017).
3. D. R. G. Achar, J. Ruge and S. Sundaresan, Aluminium **6** (56), 391-397 (1980)
4. H. Laukant, „Laserschweiß-Löten von Stahl-Aluminium-Mischverbindungen", Ph. D. thesis, Universität Bayreuth, 2007.
5. L. Agudo and N. Jank, steel research international **7**, 530-535 (2008).
6. U. R. Kattner and T. B. Massalski in *Binary Alloy Phase Diagrams* (H. Baker, Ohio, 1990), p. 147.
7. H. Springer and A. Kostka, Acta Materialia **59**, 1586-1600 (2011).
8. N. Yamamoto and M. Takahashi, Materials Science Forum **539-543**, 3865-3871 (2007).
9. A. Ambroziak, M. Korzeniowski, P. Kustron, M. Winnicki, P. Sokolowski and Ewa Harapinska, Advances in Materials Science and Engineering **2014**, 1-15 (2014).
10. N. Jank, H. Staufer and J. Bruckner, BHM **153** (5), (2008).
11. F.-W. Bach and K. Lau, Aachener Berichte Fügetechnik, 461-475 (2007).
12. S. E. Thürer, J. Uhe, O. Golovko, C. Bonk, A. Bouguecha, C. Klose, B.-A. Behrens, H. J. Maier, AIP Conference Proceedings **1896**, 140002 (2017).
13. B.-A. Behrens, C. Klose, A. Chugreev, N. Heimes, S. E. Thürer and J. Uhe, Metals **8**, 1-14 (2018).
14. S. Herbst, C. N. Dovletoglou and F. Nürnberger, Metallography, Microstructure, and Analysis **6**, (2017).
15. G. Rummel, T. Zumkley, M. Eggersmann, K. Freitag and H. Mehrer, Zeitschrift für Metallkunde **95a**, (1995).